J. Phys. Chem. Solids, 1975, Vol. 36, pp. 229–238. Pergamon Press. Printed in Great Britain

LCAO TRUNCATED CRYSTAL CALCULATIONS ON SOME ELECTRONIC PROPERTIES OF

ALEX ZUNGER

(*Received* 15 *October* 1973)

Abstract. The truncated crystal method is used to describe the band gap, work function, repulsive ground state crystal potential, Davydov excitons and defect states due to H and N impurities in molecular P-2 hydrogen crystal.

1. INTRODUCTION

The truncated crystal approach to the description of electronic properties of covalent solids, has been successfully applied in recent years to a large variety of problems[1–6]. This method, characterized by solving for

LCAO representation or by Slater's $X\alpha$ method[7] and

boundaries are either periodic connections[5, 8, 9] or

dangling bonds[2], has proved to be useful in several respects:

(1) when convergence limit is reached, it is possible to

localized point defect states as well as electronic

theory[10] and defect molecule[11] approaches to the

of density and of properties of clusters where a guest atom or molecule with different electronegativity than the host crystal, has been substituted[5].

These advantages of the truncated crystal approach are used in this paper to calculate various electronic properties of molecular hydrogen crystals.

Much theoretical effort has been devoted lately to the investigation of properties of compressed solid hydrogen at low temperatures, mainly due to the interesting possibility of producing a high pressure phase of metallic hydrogen in the laboratory[12, 14], and because of interest in laser production of hydrogen plasma from cold solid hydrogen, for use in thermonuclear reactions[15]. The former problem, treated from the point of view of metal–insulator transition, requires the knowledge of the

one-electron energy states in the molecular phase with

optical frequencies by the cold solid hydrogen, which is

questions involving the density dependence of electronic properties, namely: to what extent it is possible to lower the ionization potential and the lowest singlet–singlet excitation energy (band gap) of the solid (which are both

suggested to lower the energy of the first electronic

impurities (H, H_2) exist like the molecular solid, thereby

states and their separation from the bottom of the conduction band.

In Section 2 we describe the molecular cluster method and specify the quantum mechanical methods that are used with it. In Section 3 we treat some one-electron states in the crystal (corresponding to energies of ionization and edge of conduction band) and in Section 4 the Frenkel exciton states are discussed by the same method. In Section 5 we present some model calculations on impurity states in solid hydrogen.

2. DESCRIPTION OF THE MOLECULAR CLUSTER MODEL

The electronic wave functions of a crystal in the LCAO approach are given by:

$$\phi_i = \sum_{\nu=1}^{N} C_{\nu i}\chi_\nu \qquad i = 1, 2 \ldots N \tag{1}$$

where χ_ν denote the atomic orbitals on site ν. The $C_{\nu i}$ are the solutions to the one-electron Hartree–Fock equations for the crystal, given by:

$$\sum_{\nu=1}^{N}$$

The ϵ_i are the one-electron crystal orbital energies, $F_{\mu\nu}$ are the matrix elements of the one-electron effective Hamiltonian in the frame of the atomic orbitals and $S_{\mu\nu}$ are overlap integrals between these atomic orbitals. We

also be interested in correlating the properties of the crystal orbitals belonging to the localized defect state with states of the ideal crystal. Therefore, instead of factorizing the secular problem (2) by considering translational symmetry, we propose to solve (2) directly under some simplifying assumptions on $F_{\mu\nu}$ as a function of N, for

the one perturbed by a point defect, as N as increased.

various densities, through a charge self-consistent solution of (2), thereby providing a simple density description of these properties. This truncated crystal approach was previously applied to lattice dynamic properties of atomic solids[18, 19] and to electronic properties of atomic[1–6] and molecular[20] solids.

The matrix elements $F_{\mu\nu}$ are approximated either by the

diagonal matrix element are given by:

$$F_{\mu\nu} = S_{\mu\nu}[H_{\mu\mu}(Q_\mu) + H_{\nu\nu}(Q_\nu)] \times (1 - 0{\cdot}5|S_{\mu\nu}|) \tag{3}$$

dependent through the relation

$$H_{\mu\mu}(Q_\mu) = H^\circ_{\mu\mu} + Q_\mu \Delta_\mu \tag{4}$$

and $H^\circ_{\mu\mu}$ is the Hartree–Fock free atom one-electron orbital energy for the μth orbital, and Δ_μ is the change in orbital energy per unit charge. A minimal basis set of Slater orbitals is employed. For hydrogen 1s state, $H^\circ_{\mu\mu}$ is taken as $-13{\cdot}6$ eV and Δ_μ as $-14{\cdot}0$ eV[22]. $S_{\mu\nu}$ are calculated using Slater orbitals with the best variational exponent of 1·2. After obtaining an initial guess for the

assuming the experimental $Pa3$ structure. The clusters are formed by taking a central molecule and adding successive shells of neighbours (13, 18, 43, 55, 77 molecules for 1, 2, 3, 4, 5 orders of neighbours, respectively). Since we are not interested in the properties of the small clusters themselves, the intermolecular distances are taken to be the bulk values with no relaxations allowed. The coefficients $C_{\nu i}$ are then used to calculate the net atomic charges Q_μ for all the atoms and the cycle repeated until convergence of 0·005 e is obtained between successive iterations. The atomic charges are computed from one and two center contributions to the charge moments by a procedure that leaves the projection of the centroid of charge, onto the line connecting the two atoms,

the atoms involved have different electronegativities.

The one-electron energy levels obtained, are populated with N electrons and the band gap is defined as the difference between highest occupied and lowest vacant cluster states, while the Koopman's cluster ionization potential is taken as the negative of the energy of the

closely related to the Cusacks approximation employed

this method provides a reasonable approximation. In the limit of an isolated H_2 molecule, at experimental equilibrium internuclear separation, this procedure yields a ionization potential of 15·38 eV compared with the experimental[26] value of 15·43 eV, an $X^1\Sigma_{1g}$ to $B^1\Sigma_{1u}$ one-electron energy gap of 10·965 eV as compared with

value of 4·66 eV as compared with the experixntal value of 4·474 eV[26].

In the INDO approach, the off diagonal matrix element is taken as

$$F_{\mu\nu} = \beta^\circ_{AB} S_{\mu\nu} - \tfrac{1}{2} P_{\mu\nu}\gamma_{AB} \tag{5}$$

and the diagonal elements are

$$F_{\mu\mu} = U_{\mu\mu} + (P_{AA} - \tfrac{1}{2}P_{\mu\mu})\gamma_{AA} + \sum_{B \neq A}(P_{BB}\gamma_{AB} - V_{AB}) \tag{6}$$

where the bonding parameter β°_{AB} is determined empiri-

cally to give an overall best fit to accurate LCAO–SCF

Roothaan[27]. When the electron repulsion integrals are

formulation (equations 5–6) of Pople *et al.*[23], and used the INDO approach in truncated crystal calculation only to a limited extent, due to its failure to account reasonably for the free molecule properties (although different parametrization schemes could produce a better agreement).

IN SOLID Pa3 HYDROGEN

Figure 1 represents the calculated band gap and ionization potential for $Pa3$ clusters of increasing number of molecules as obtained in the truncated crystal calculations with IEXH calculations. For 3 orders of neighbours, convergence is obtained even for the highest density

occupied crystal orbital energies) and ionization potential

form clusters, and further decrease is obtained as the

band is probably not adequately described by the minimal basis set employed, and since this description becomes

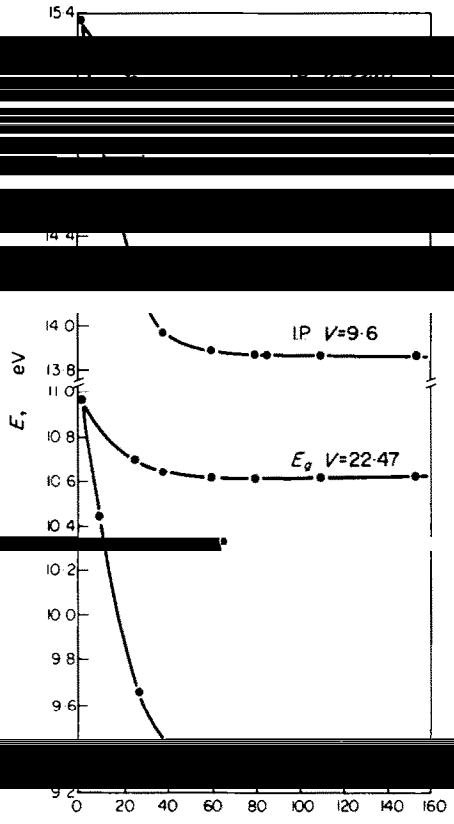

Fig. 1. Variation of ionization potential (*IP*) and band gap (E_g)

valence band, no attempt was made to further increase the density of the cluster towards the metal hydrogen limit.

The convergence of the band gap and ionization potential as a function of cluster size, as obtained by applying the INDO approximation to the matrix elements

as already noted, yields poor agreement even with isolated molecule experimental data for these properties, the values obtained for cluster calculation are not of much interest, and we will proceed with the IEXH approximations to

mentioning that the relative decrease in ionization potential and band gap, as a function of cluster size, is similar in both methods, indicating that cluster models of this size are probably sufficient to describe these properties in the bulk.

Since the charge distribution over the atoms in the molecular cluster was relatively homogeneous even at the clusters surface (contrary to the situation in clusters nitride[5a] and diamond[2, 4] where the bonded atomic interactions tend to accumulate excess charge on the unsaturated atoms at the surface), no attempt has been made to apply periodic boundary conditions to suppress charge inhomogeneity. This however would probably be important in similar studies on atomic hydrogen crystals[28].

In Fig. 3, the density dependence of some calculated electronic properties of solid $Pa3$ hydrogen is revealed, as obtained in the cluster calculation with IEXH approxima-

corresponding to the free molecule values, coincide with the values obtained by the same method of calculation for a single molecule. For the experimental equilibrium volume ($V = 22{\cdot}47$ cm^3/mole, $a = 5{\cdot}2875$ Å) the band gap in the cluster is 10·7 eV, as compared with the lower edge of the singlet–singlet absorption of solid D_2 obtained by Baldini[29] in the u.v. spectrum, of 10·8 eV. For the highest density considered ($V = 9{\cdot}6$ cm^3/mole), the gap

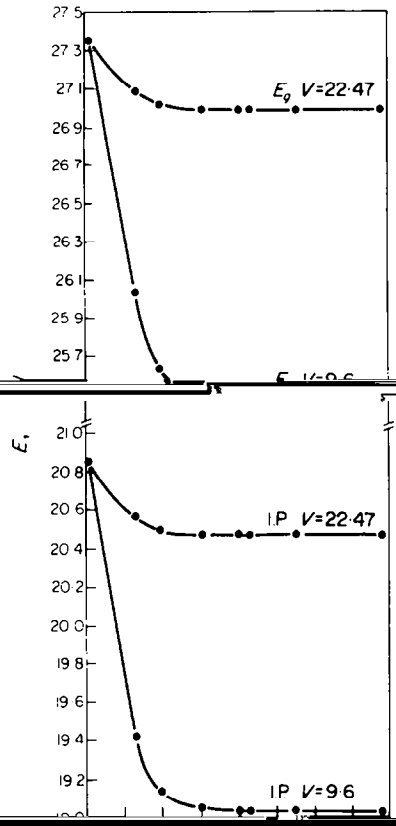

Fig. 2. Variation of ionization potential (*I.P.*) and band gap (E_g) with cluster size for two volumes (V in cm^3/mole) as calculated for INDO clusters.

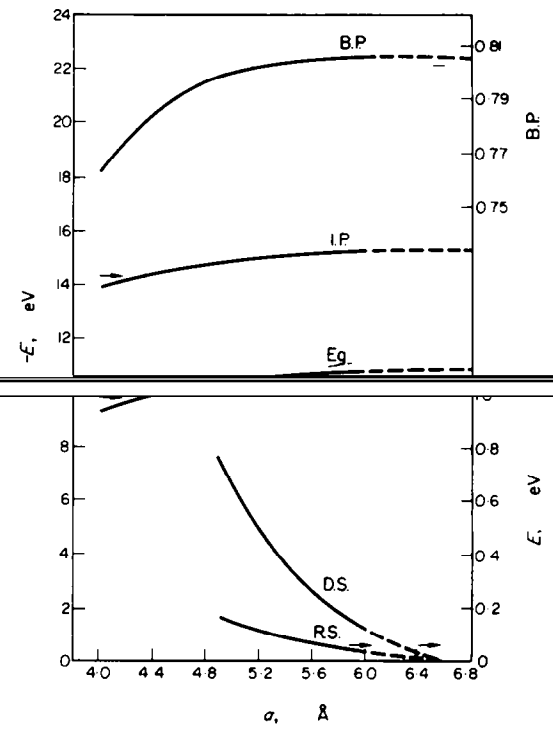

Fig. 3. Density dependence of several electronic properties at the convergence limit, calculated by IEXH method. *B.P.*: bond population, *I.P.*: ionization potential, E_g: band gap, *D.S.*: Davydov

decreases to 9·2 eV*. It is also observed that the decrease in the band gap is mainly due to the decrease of the energy

that are lower than those obtained by the molecular cluster approximation, reaching at the limit of very low density to an overestimation of 5·6 eV of the experimental ionization potential. This large deviation both from experimental results at very low densities and from the

equilibrium volume and rises to 4·94 eV at V = 9·6 cm^3/mole.

An attempt to calculate electronic energy changes in solid molecular hydrogen due to density changes, was previously made by Chapline[13]. The change in one-electron energy from that in a hydrogen molecule was

metallic forms[13, 14].

The binding energy per molecule, is calculated in the cluster model by summing the one electron energy levels of all occupied states. Since LCAO treatment of closed shell systems reveals only the repulsive potential[30, 31] (unless configuration interaction is introduced), the excess

function outside the molecular Wigner–Seitz sphere. Extending this calculation to lower densities, shows that the Wigner–Seitz model results in one-electron energies

of our cluster calculation with the phenomenological form of pair interaction

$$\phi_{rep} = 4\epsilon\left(\frac{\sigma}{r}\right)^{12} \tag{7}$$

we get for 3·70 Å $< r <$ 3·80 Å, taking the accepted value

*This decrease in excitation energy upon compression is probably too low for increasing significantly the absorption

as compared with the experimental value of the bulk

cluster approximation, was previously obtained also for N_2–N_2 interaction[20].

A different representation of the interaction in the crystal could be obtained by calculating the change in

the strength of the molecular bond at various crystal densities. It is evident that upon compression of the unit cell, keeping the molecular bond length constant, this bond is weakened due to extraction of electronic charge from the region between two bonded hydrogen atoms.

4. FRENKEL EXCITONS IN HYDROGEN Pa3

We next consider the energies of the Frenkel exciton states in molecular solid hydrogen by the same LCAO approach.

factor group. A group theoretical analysis reveals that the free molecule (point group $D_{\infty h}$) ground state $^1\Sigma_g$ yields in the T_h factor group a totally symmetric representation

tion in the factor group. The A_u state is optically inactive, while the transition to the triply degenerate T_u state is dipole allowed and polarized along the x, y, z unit cell directions. The transition to the free molecule zero vibrational state of $B^1\Sigma_{1u}$ occurs at 11·235 eV[26] and at

of solid D_2 at 6°K[29] reveals an absorption edge at 10·8 eV originating from the same molecular transition, followed by a relatively broad absorption band peaking at about 12 eV. At higher energies this absorption overlaps with the lower part of the $2p\,^1\Pi_u$ absorption. The energy

site i of unit cell n ($i = 1, 2, 3, 4$, $n = 1, 2 \ldots N$) by ϕ^s_{ni} and ϕ°_{ni} for the lowest excited singlet and the ground electronic state respectively, a straight forward Frenkel formalism yields for the $Pa3$ group, the energies of the

as

where

$$\ldots \qquad (10)$$

$\Delta\epsilon^s$ is the free molecule excitation energy to state s and $V_{ni,mi}$ is the intermolecular potential (in equation 10 the double indices are suppressed). Molecule 1 at the origin of

$\lambda = 1$ is of A_u symmetry while the states $\lambda = 2, 3, 4$ belong to the triply degenerate T_u representation. Since for dipole allowed states in the $Pa3$ structure, all $L_{ni,01}$ are equal, we denote $J' = L_{ni,01}$ for $\lambda = 2, 3, 4$ and $J = L_{n1,01}$, adopting the notation of Hexter for vibrational excitons[36]. The splitting between the T_u and A_u states

$(D^s + J)$.

The energies of the exciton states will be evaluated in

direct solution of the LCAO problem for H_2 dimers oriented mutually as pairs in the crystal; (b) expansion of the $L_{ni,01}$ matrix elements in multipole series and retention

excited state.

(a) The splitting between the excited states of a H_2 dimer formed from molecules 1 and 2, is twice the

and the sum in equation (9) evaluated directly for n ranging to 6 orders of neighbours. The dimers one-electron energies are computed by IEXH method (equation 3) with the atomic parameters mentioned in Section 2. This yields at normal density, a splitting of

and T_g states at $\vec{K} = 0$) is similarly calculated to be 1·22 eV.

The additivity of pair interactions is checked, in the nearest neighbour approximation by comparing the splitting yielded by equation (9) when n is extended to

obtained agree with each other within 2%–4% in the density range between 22·47 cm^3/mole and 17·5 cm^3/mole. This is a measure for non additivity corrections in this model.

the band relative to the free molecule transition is

performing a cluster calculation on one molecule surrounded by 5 orders of neighbours and analyzing the resultant one-electron energy levels to obtain the shift of the band. The result of the first calculation is −0·10 eV while the cluster calculation reveals a shift at −0·093 eV. Higher order perturbation terms corresponding to different polarizations of the crystal by the ground and excited state are difficult to calculate and could be important in determining the Davydov shift. The experimental shift of the center of the absorption band in D_2[29] is approxi-

mental value by a factor of 2–3, due to the neglect of other than dipole interactions and relaxation effects.*

Mixing of the T_u exciton component with other T_u states originating from the free molecule dipole allowed $^1\Pi_u$ state or the octupole allowed $^1\Delta_u$ state are possible via second order crystal field effects, but will probably affect the splitting only to a small extent due to the large value of the oscillator strength to the $B^1\Sigma_{1u}$ state.

When the calculation of the splitting in the semiempirical LCAO approach is performed for various crystal

(b) A different approach to evaluate the energies of the dipole allowed exciton states rests upon expanding the interaction potential in multipole series and retaining only the first non-zero moment. Equation (9) in this approxima-

cell dimension a as $a^{-8\cdot1}$ (Fig. 3) over the range $5\cdot2 \leq a$ $4\cdot9$ Å, which is a much stronger dependence than that anticipated by pure dipole interactions. This short range character results from the description of intermolecular

rapidly with distance. Similarly, the Davydov splitting

a dependence of $a^{-12\cdot7}$ which is also much shorter range

and λ are integers. If we denote the orientation of each sublattice by unit vectors $\hat{e}_i$, the angles are defined by:

potentials, respectively.

The number of pairs of states joining the valence and conduction levels respectively in the energy between $\hbar\omega$

(12)

and M^s is the molecular electronic transition dipole related to the absorption oscillator strength f by

$$|M^s|^2 = \frac{3he^2 f}{8\pi^2 m_e c\bar{\nu}} \tag{13}$$

where m_e is the electron mass and $\bar{\nu}$ is the frequency at the center of the band. For an f.c.c. lattice, the sum in equation (11) can be easily evaluated by the Nijboer and de

frequency and f as the gas phase total oscillator strength

description is possible. Figure 4 describes this joint density of states, as obtained by sampling the clusters orbital energies. The edge of the absorption is now of T_u character and appears at 10·5–10·6 eV as compared with the experimental value of Baldini[29] for D_2 crystal, of 10·8 eV. The region above ≈11·3 eV, is of A_u character and the transition to it is forbidden. The qualitative overall shape of the spectrum is similar to the observed absorption, though quantitatively the calculated spectrum is slightly narrower, probably due to the neglect of the

the spectrum

between A_u and T_u a value of 0·15 eV which is considerably lower than the value obtained by the LCAO cluster calculation, employing the full interaction. Splitting calculated according to dipole transition moments were shown in other cases to underestimate the experi-

isolated H_2 molecule and the solid, was estimated from the electronic spectrum of large radius Wannier impurity states in X_e/H_2 system[42] and in pure H_2[43]. The impurity ionization potential in solid inert medium $IP_{im}(s)$ is related to the gas-phase impurity ionization

one postulated by Hexter[38]), yields in the dipole approximation

$$IP_{im}(s) = IP_{im}(g) + P_+ + V_+ \tag{14}$$

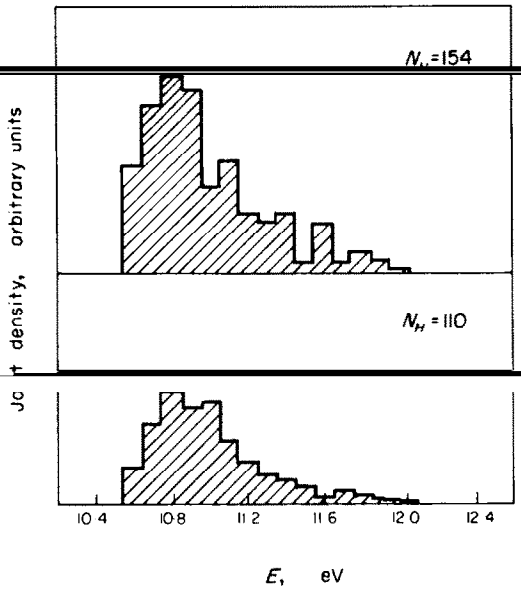

Fig. 4. Transition density of states (number of states connecting valence and conduction bands, respectively within energy range from E to $E + \Delta E$) as a function of energy, as calculated by IEXH for the 110H and 154H clusters.

energy of the medium and V_0 is the energy of the quasi free electron state corresponding to the bottom of the conduction state relative to the vacuum level. Similarly, the pure solid ionization potential $IP(s)$, is related to the ionization potential of its free constituents $IP(g)$, by [42]:

$$IP(s) = IP(g) + P_+ + V_0 + E_c \qquad (15)$$

where E_c corresponds to the energy difference between the [illegible]

X_e/H_2 system [42] together with the knowledge of the experimental value of $IP_{im}(g)$ for X_e, suggests that $-(P_+ + V_0) \sim 1$–2 eV in solid H_2, which yields, through equation (15), taking $IP(g) = 15{\cdot}43$ eV [26], on a ionization potential for the solid of $[13{\cdot}5$–$14{\cdot}5 + E_c]$ eV $\approx$ 14·1–15·1 eV. Evidence for a possible convergence limit of the Wannier series at 14·4 eV in pure solid H_2 [43]

Simple theoretical calculations of P_+ [42] based on the

liquid H_2, and with the spectroscopic value of $V_0 =$ [illegible] repulsive pseudopotential that was taken to depend semi-empirically on the scattering length.

5. POINT DEFECTS IN SOLID H_2

The relatively large band gap and ionization potential of solid H_2 [illegible] almost exclude processes such as simple bound optical transitions to conduction or ionized states, under conditions of irradiation with laser photons of energy in the range of 1–2 eV, as desired in experiments of laser heating of solid H_2 [15, 48]. Multiphoton mechanisms [49] or generation of antistokes radiation inside the target [50] are not sufficient to enhance these absorption processes sufficiently. Another possible way of lowering the effective energy gap for such transitions, is introduction of impurities inside the solid target, thereby creating allowed electronic states in the otherwise forbidden gap. The truncated crystal method described in Section 2 was demonstrated to be suitable for calculation of such states in covalent crystals [2–6] because it provides a simple means of correlating the one-electron energy states of localized impurities with respect to the band edges. Employment of charge self-consistent methods to calculate the one-electron energy states of a cluster containing an impurity with different electronegativity than that of the host atoms, and the allowance made for small lattice distortions and relaxations around the center, provide useful mechanisms for introducing charge and energy redistribution effects that are important in problems of deep impurity states [4, 5].

We chose to discuss here some model calculations for two impurities that may enter unpurified solid hydrogen: an isolated hydrogen atom and a nitrogen molecule. The procedure of calculation goes in the following steps: (a) We choose a large enough hydrogen molecular cluster so that the examined (Section 3) electronic properties [illegible]

the origin +3 shells) exhibits a band gap, ionization potential, average charge per atom and overlap population between two bonded atoms, very close to that of the convergence limit defined as that of the largest cluster considered (Fig. 1).

(b) The central H_2 molecule at the origin is then replaced by the chosen impurity and the calculation of the

the cluster size from 3 to 4 and 5 shells of H_2 molecules

(c) Once the one-electron energy levels associated with [illegible] small ($\Delta = 0{\cdot}1$–$0{\cdot}2$ Å) relaxations of the lattice around the guest molecule, in directions parallel to the body diagonals of the $Pa3$ unit cell, in order to examine the effect of model distortions on the defect states.

1. *Hydrogen atom impurity*

Table 1 summarizes the main results obtained for the H atom defect.

The energy of the impurity states is shown to become stable relative to the band edges, resulting in a net destabilization of the atomic 1*s* state of hydrogen relative to the free atom. The one-electron energy state corres-

vicinity of the atom, exerting only small perturbation on the charge distribution of the neighbouring molecules

accumulates a net electron density on it of the order of $-0{\cdot}02\,e$. Inward relaxations of the lattice result in a relative destabilization effect on the defect state, while outward relaxation tend to stabilize it. It should, however, be kept in mind that the cluster model suggested does not represent adequately the real restoring forces of the covalent molecular crystal due to the lack of second order polarization forces in this closed shell LCAO picture. Calculations of equilibrium positions of the surrounding

As the unit cell dimension a of the crystal is decreased, (Fig. 5) the impurity level approaches the edge of the conduction band being for instance already 8·7 eV from it at $a = 5{\cdot}0$ Å. The net charge accumulated on the defect atom rises also with decreasing unit cell dimension, and

2. *Nitrogen molecule impurity*

An isolated N_2 molecule is described in the IEXH frame (free atom orbital energies taken from Hartree–Fock calculation on the ^4S ground state[51] and charge dependent energies form the work of Rein *et al.*[22]) to have an equilibrium internuclear distance of 1·15 Å (experimental value 1·098[26]) a $2\sigma_g$ ionization potential

tion energy of 9·9 eV (experimental value 9·756 eV[26]) and a bond population of 1·675. The lowest vacant orbital

molecule is placed at the origin of the $Pa3$ molecular hydrogen cluster and calculation steps (a)–(c) performed. The results are shown in Table 2.

The π_g orbital remains unsplit in the crystal and appears in the band gap. The lowest $2\sigma_g \rightarrow \pi_g$ molecular transition is blue shifted relative to the transition in the isolated molecule by 0·18 eV at normal density. Both $2\sigma_g$ and the π_g levels are stabilized in the crystal relative to their free molecule positions while smaller stabilizing

molecular orbital energies.

Again the guest molecule has only a small perturbative effect on the charge distribution around it, at normal density, and the nitrogen molecular bond population decreases slightly with respect to the free molecule value.

Table 1. Energy states of conduction and valence band edges and impurity state for relaxed ($\Delta = 0{\cdot}2$ Å) and unrelaxed lattice for the H-impurity clusters

			Impurity state (eV)		
Cluster	Conduction edge (eV)	Valence edge (eV)	No relaxation	Inward relaxation	Outward relaxation
I + 36	4·451	15·098	13·419	13·398	13·578
I + 42	4·455	15·065	13·418	13·399	13·580
I − 54	4·456	15·065	13·417	13·399	13·580
I + 76	4·456	15·063	13·417	13·399	13·580

Table 2. Energy states of conduction and valence band edges and impurity state for relaxed ($\Delta = 0{\cdot}2$ Å) and unrelaxed lattice for the N_2 impurity clusters

			π_g Impurity state (eV)		
Cluster	Conduction edge (eV)	Valence edge (eV)	No relaxation	Inward relaxation	Outward relaxation
I + 36	4·447	15·094	11·099	11·030	12·050
I + 42	4·455	15·066	11·098	11·032	12·052
I + 54	4·456	15·065	11·098	11·033	12·054
I + 76	4·456	15·065	11·098	11·034	12·054

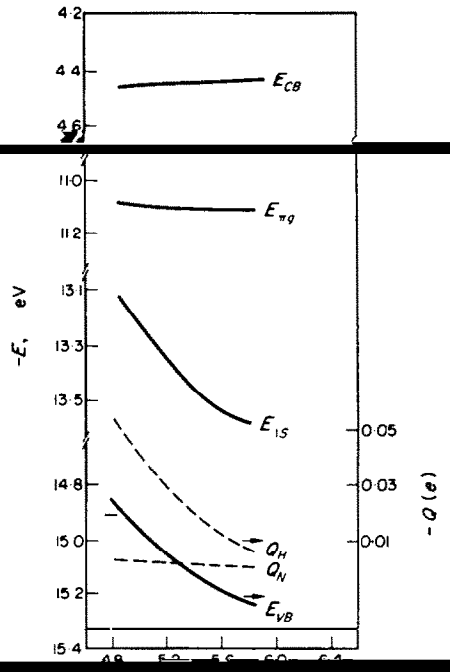

Fig. 5. Variation of some electronic properties for the defect crystal problem. E_{CB} and E_{VB}: energies of the edge of conduction and valence bands respectively (with N_2 impurity). E_{π_g}: one electron defect state of $N_2 \pi_g$ level, E_{1_s}: one electron defect state of H 1S level Q_H, Q_N: net atomic charges of H and N atoms in the cluster.

increases slightly in absolute value, on expense of the less electronegative hydrogen molecules surrounding it. Relaxation of the lattice around the impurity molecule results in relatively small shifts of the impurity level.

6. SUMMARY

We have used the truncated crystal approach with an [illegible] density of states of molecular hydrogen clusters, for several densities, as a function of cluster size for "spherical" clusters. Information regarding density effects on charge distribution and one electron energy [illegible] ideal crystal and model impurity states due to hydrogen atom and nitrogen molecule, are investigated. The main advantages of the method lie in its ability to treat ideal crystal states as well as localized defect states in a unified model when the convergence limit is reached and in the simple way of introducing self-consistent charge redistribution and relaxation effects. The main shortcomings of lack of configuration interaction in the calculation, which are both presently excluded due to limitation in computer storage.

Acknowledgements—The author would like to thank Prof. I. Jortner for many helpful discussions and advice. Professor R. Engelman is gratefully acknowledged for critical reading of the manuscript.

REFERENCES

1. Moore E. B. and Carlson C. M., *Solid State Commun.* **4**, 47 (1965).
2. Larkins F. P., *J. Phys. Chem.* **4**, 3065, 3077 (1971).
3. Zunger A., *Solid State Commun.* **11**, 1717 (1972).
4. Messmer R. P. and Watkins G. D., *Phys. Rev. Lett.* **25**, 656 (1970); *Phys. Rev.* **B7**, 2568 (1973).
5. Zunger A., *J. Phys. C* (a) 7, 76 (1974), (b) 7, 96 (1974).
6. Hayns M. R., *Phys. Rev.* **B5**, 697 (1972), also *J. phys. Chem.* **5**, 15 (1972).
7. Johnson K. H., *J. de Phys.* C3, 195 (1972).
8. Watkins G. D. and Messmer R. P., in *Computational methods for large molecules and localized states in solids* (edited by Herman F., McLean A. D. and Nesbet R. K.) p. 133. Plenum Press, New York (1973).
9. Messmer R. P. and Watkins G. D., in *Radiation damage and defects in semiconductors*, Conference Series No. 16, p. 255.
11. Coulson C. A. and Kearsley M. J., *Proc. R. Soc. Lond.* **A241**, 433 (1957).
12. Dynin E. A., *Sov. Phys. Solid State* **13**, 2089 (1972).
13. Chapline G. F., *Phys. Rev.* **B6**, 2067 (1972).
14. Neece G. A., Rogers F. J. and Hoover W. G., *J. Computational Phys.* **7**, 621 (1971).
15. Basov N. G., Krokhin O. and Sklizkev G. V., *Proc. 2nd W.S. at Renssel Polyt. Inst. Hartford*, p. 389 (1971).
16. Bruce T. A., *Phys. Rev.* **B5**, 4170 (1972).
18. McGinty D. J., *J. chem. Phys.* **55**, 580 (1971).
19. Burton J. J., *J. chem. Phys.* **52**, 345 (1970).
20. Zunger A., *Mol. Phys.* **28**, 713 (1974).
21. Cusachs L. C. and Reynolds J. W., *J. chem. Phys.* **43**, S160 (1965).
22. Rein R., Fukuda H., Win H., Clark G. A. and Harris F. E., *Quantum aspects of heterocyclic compounds in chemistry and*
24. Blyholder G. and Coulson C. A., *Theor. Chim. Acta.* **10**, 316 (1968).
26. Herzberg G., *Diatomic molecules*, University Press, Van Nostrand, Princeton, New Jersey (1950).
27. Roothaan C. C. J., *J. chem. Phys.* **19**, 1445 (1951).
28. Zunger A., unpublished.
29. Baldini G., *Jap. J. App. Phys.* **4**, Suppl. I. 613 (1965).
30. Margenuu H. and Kestner N. R., *Theory of intermolecular forces*, Pergamon Press, Appendix A (1969).
31. Salem L., *J. Amer. chem. Soc.* **90**, 543 (1968).
32. Michels A. M., de Graaf W. and ten Seldam C. A., *Physica* **26**,

36. Hexter R. M., *J. chem. Phys.* **36**, 2265 (1962).
37. Nijboer B. R. A. and de Wette F. W., *Physica* **24**, 422 (1958); *ibid.* **24**, 1105 (1958).
38. Hexter R. M., *J. chem. Phys.* **37**, 1247 (1962).
39. Grigas J. and Tamashevskiy V., *Z. Naturforsch.* **21a**, 626 (1966).
Phys. **38**, 510 (1960).
41. Roith M. and Schnepp O., *Mol. Phys.* **9**, 473 (1965).
(1972).
43. Gedanken A., Raz B. and Jortner J., *J. chem. Phys.*
45. Mott N. F. and Littleton M. J., *Trans. Faraday. Soc.* **34**, 485 (1938).
46. Springett B. E., Cohen M. H. and Jortner J., *J. chem. Phys.* **48**, 2720 (1968), *ibid.* **51**, 2291 (1969).
47. Halpern B. and Gomez R., *J. chem. Phys.* **51**, 1031 (1969).
49. Bebb H. B. and Gold A., *Phys. Rev.* **143**, 1 (1966).
50. Mennicke H., *Phys. Lett.* **37a**, 381 (1971).
51. Clementi E., *IBM J. Res. Develop. Suppl.* **9**, 2 (1965).
52. Cederbaum L. S., Hohlneicher G. and Von Niessen W., *J. chem. Phys.* **44**, 1073 (1966).

After this paper has been accepted, two papers on the band structure of solid Be_2 Hydrogen have appeared: the work of L. A. (1973)] using a tight-binding procedure with nearest-neighbor interactions, neglecting three and multicenter integrals and *C.* **7**, 2467 (1974)] using a spherical approximation to the Columb molecular potential including three forms of exchange (Slater[a], Lundqvist-Lundqvist[b] and Khon-Sham[c]) in a non-self-consistent treatment. The following table summarizes the results:

Property	Monnier *et al.*	Gomez *et al.*	Present work	Expt.
IP (solid) eV	19·1[a] 15·5[b] 14·2[c]	15·82	15·1	14·5[f]
Band width eV	0·369[a] 0·825[b] 0·945[c]	1·1	1·22	—
Eg eV	12·029[a] 9·276[b] 8·789[c]	—	10·7	~10·8[d]
IP (molecule) eV	15·0	16·135	15·38	15·43[e]
Dissociation Energy (molecule) eV	3·488	3·488	4·66	4·474[e]

(a) Slater exchange [J. C. Slater, *Phys. Rev.* **81**, 385 (1951)].
(b) Lundqvist Lundqvist exchange [P. J. Lundqvist and S. Lundqvist, *Computational Solid*
(c) Kohn and Sham exchange [W. Khon and L. J. Sham, *Phys. Rev.* **140A**, 1133 (1965)].
(d) Ref. 29.
(e) Ref. 26.
(f) Ref. 43.

In this table, IP (solid) denotes the negative of the highest occupied valence band state (Γ_4 in the notation of Gomez *et al.* and X_1 in the notation of Monnier *et al.*) and E_g denotes the transition between the Γ_4 and Γ_4' states ($X_1 \rightarrow X_4$ in the notation of Monnier and $T_g \rightarrow T_u$ in the notation of the present paper). The
free molecule. Reasonably good agreement is obtained between the present work and the works of Gomez *et al.* and Monnier *et al.* In a
Parravicini and M. Vittori, unpublished], using a nonlocal exchange potential in the zero-overlap approximation and a Coulamb potential from the Slater 1*s* charge density, the lowest conduction state was calculated to be of Γ_1 symmetry and this state was separated by a gap of 13·8 eV from the top of the valence band. The
work (E_g = 10·7 eV) and the observed edge of the absorption edge of Baldini, 10·8 eV [29].